AIP Journal of Applied Physics

The role of confinement on stress-driven grain boundary motion in nanocrystalline aluminum thin films

Daniel S. Gianola, Diana Farkas, Martin Gamarra, and Mo-rigen He

Citation: Journal of Applied Physics **112**, 124313 (2012); doi: 10.1063/1.4770357
View online: http://dx.doi.org/10.1063/1.4770357
View Table of Contents: http://scitation.aip.org/content/aip/journal/jap/112/12?ver=pdfcov
Published by the AIP Publishing

Articles you may be interested in

Mechanical strain mediated carrier scattering and its role in charge and thermal transport in freestanding nanocrystalline aluminum thin films
J. Vac. Sci. Technol. B **33**, 022002 (2015); 10.1116/1.4906834

Thermally driven grain boundary migration and melting in Cu
J. Chem. Phys. **142**, 054706 (2015); 10.1063/1.4907272

Effect of grain size on the melting point of confined thin aluminum films
J. Appl. Phys. **116**, 164302 (2014); 10.1063/1.4899240

The effect of solute segregation on strain localization in nanocrystalline thin films: Dislocation glide vs. grain-boundary mediated plasticity
Appl. Phys. Lett. **102**, 241916 (2013); 10.1063/1.4811743

Study of the effect of grain boundary migration on hillock formation in Al thin films
J. Appl. Phys. **90**, 781 (2001); 10.1063/1.1381045

MIT LINCOLN LABORATORY CAREERS

Discover the satisfaction of innovation and service to the nation

- Space Control
- Air & Missile Defense
- Communications Systems & Cyber Security
- Intelligence, Surveillance and Reconnaissance Systems
- Advanced Electronics
- Tactical Systems
- Homeland Protection
- Air Traffic Control

LINCOLN LABORATORY
MASSACHUSETTS INSTITUTE OF TECHNOLOGY

[This article is copyrighted as indicated in the article. Reuse of AIP content is subject to the terms at: http://scitation.aip.org/termsconditions. Downloaded to] IP: 128.173.126.47 On: Thu, 07 May 2015 16:31:19

The role of confinement on stress-driven grain boundary motion in nanocrystalline aluminum thin films

Daniel S. Gianola,[1,a)] Diana Farkas,[2,a)] Martin Gamarra,[2] and Mo-rigen He[1]
[1]*Department of Materials Science and Engineering, University of Pennsylvania, Philadelphia, Pennsylvania 19104, USA*
[2]*Department of Materials Science and Engineering, Virginia Tech, Blacksburg, Virginia 24061, USA*

(Received 23 September 2012; accepted 19 November 2012; published online 21 December 2012)

3D molecular dynamics simulations are performed to investigate the role of microstructural confinement on room temperature stress-driven grain boundary (GB) motion for a general population of GBs in nanocrystalline Al thin films. Detailed analysis and comparison with experimental results reveal how coupled GB migration and GB sliding are manifested in realistic nanoscale networks of GBs. The proximity of free surfaces to GBs plays a significant role in their mobility and results in unique surface topography evolution. We highlight the effects of microstructural features, such as triple junctions, as constraints to otherwise uninhibited GB motion. We also study the pinning effects of impurities segregated to GBs that hinder their motion. Finally, the implications of GB motion as a deformation mechanism governing the mechanical behavior of nanocrystalline materials are discussed. © *2012 American Institute of Physics*. [http://dx.doi.org/10.1063/1.4770357]

I. INTRODUCTION

Nanocrystalline (NC) metals and alloys have shown many enhanced mechanical properties compared to their coarse-grained counterparts,[1–6] and their mechanical response is thought to be strongly influenced by the large fraction of material residing at or near grain boundaries (GBs).[7–10] Plastic deformation is augmented as GBs are widely considered to serve as both promoters and obstacles to dislocation motion.[11–18] Despite the thermodynamic penalty of the large interfacial area,[19–24] many experimentally synthesized NC metals (even nominally pure ones) demonstrate remarkable thermal stability,[25–28] and such stability has been attributed to both kinetic[29–32] (e.g., GB solute drag) and energetic[33–36] (e.g., reductions in GB energy due to solute segregation) factors.

Even with the potential for thermal stability in NC metals, emerging evidence has indicated that the large stress that these materials incur prior to failure can serve as a driving force for grain growth.[37–44] Such mechanisms leading directly to plastic deformation were first experimentally shown in 1957 by Li *et al.*[45,46] to be active during room temperature deformation of materials possessing low-angle GBs. Extensions to high-angle GBs where a dislocation-based description[47] is incomplete, however, have been the subject of more recent research.[48–52] Experiments showing stress-driven grain growth[38] and GB migration[37] in NC metals at low homologous temperatures suggest that diffusive processes play a minimal to negligible role, while molecular dynamics (MD) simulations of symmetric tilt GBs[53–55] corroborate a theory by Cahn and Taylor,[56,57] wherein GB migration (normal motion) directly couples to shearing along the GB, described by a factor β that depends on GB character.[58] Atomistically, such coupled motion is ascribed to distortions and rotations of local GB structural units and the collective military motion of the boundary was reported to be athermal.[54,57] At high temperatures, coupled motion was shown to be replaced by GB sliding as the predominant response to applied shear.[57]

Despite a growing understanding of stress-driven GB migration, extensions of this theory to the realistic GB networks present in bulk and thin film NC metals, which include the role of microstructural confinement features (such as triple junctions[59] and impurities[60,61]) and accommodation mechanisms, are still limited. Rupert *et al.* recently reported room temperature micro-tensile testing and detailed microstructural characterization of NC Al thin films with intentionally patterned stress concentrators and showed that regions in the film with enhanced shear stresses demonstrated the most grain growth,[62] corroborating the theory of shear-coupled GB motion.[56,57] In similarly synthesized Al thin films, Gianola *et al.* showed that stress-driven grain growth produced surface topography evolution in the form of measurable step heights and rotations between neighboring surface grains.[63] A detailed picture of microstructural events occurring sub-surface, however, is necessary to understand the efficacy of this mechanism in the presence of constraints. Velasco recently showed via MD simulations that a buried $\Sigma 75$ symmetric tilt GB, as part of a polycrystal network, is still able to migrate by coupled motion with a value of β similar to that obtained in bicrystal simulations.[64] However, it is still not understood how more general GBs that may not be described by coincident site lattices or possess twist character will respond to applied stresses.

In the present work, we investigate the relationship between stress-driven GB motion in NC Al thin films and the presence of microstructural confinement features as is common in realistic geometries.[62,63] Surface topography evolution of deformed Al films obtained by MD simulations are compared with experiments with similar geometries and loading conditions, which provide insight to the microstructural mechanisms governing motion of a nominally random distribution of stressed GBs. Computer simulations are also used to examine

[a)]Authors to whom correspondence should be addressed. Electronic addresses: gianola@seas.upenn.edu and diana@vt.edu.

 © 2012 American Institute of Physics

[This article is copyrighted as indicated in the article. Reuse of AIP content is subject to the terms at: http://scitation.aip.org/termsconditions. Downloaded to] IP: 128.173.126.47 On: Thu, 07 May 2015 16:31:19

two potential effects on GB motion and ensuing grain growth: (1) proximity of the free surface to GBs and the constraints from triple junctions and (2) introducing impurities segregated to GBs to hinder the grain growth process.

II. COMPUTATIONAL METHODS

MD simulations were performed on a large-scale parallel supercomputer system (Virginia Tech's System X) to impose strain controlled, constant strain rate tensile deformation on virtual NC samples at various temperatures. The MD implementation is that of LAMMPS,[65] using a Nose-Hoover thermostat and barostat with a time step of 1 fs. Similar to our previous work in NC metals,[66] the digital samples were created using the Voronoi construction using random grain orientations and were subsequently relaxed to find the equilibrium atomic structures following 100 ps at 300 K. The sample contained 15 grains with sizes of approximately 14 nm. The interatomic potentials employed were those of Ruda *et al.*[67] which account for the interaction of H interstitial solute atoms in Al. To address the effects of H interstitials, two identical samples were utilized. One was pure Al and the other contained 1 at. % of H interstitials, which were all located at GBs. The samples were again relaxed to reach equilibrium GB structures following H atom incorporation. In order to understand the influence of the free surface on deformation and GB motions, another identical sample was created (with the same 15 grains and exactly the same misorientation) but positioning the free surface at a different place in the microstructure (we refer to this as "simulated polishing").

Strain controlled virtual tensile testing was then performed using periodic boundary conditions in two of the in-plane directions and a free surface boundary condition in the third direction. The dimensions other than the strained and free surfaces are controlled by a zero pressure condition. These simulations yielded stress-strain curves, atomic positions, and local atomistic quantities.

III. RESULTS

A. Surface topography evolution during stress-driven grain growth

We begin by comparing the MD results with a recent experimental study[63] showing that NC Al freestanding thin films (with thicknesses of 150 and 300 nm and mean grain sizes of 50 and 100 nm, respectively) exhibited unique surface topography following quasi-static tensile testing at room temperature. The topography evolution as characterized by steps at GBs and rotations between adjacent grains was found to correlate with stress-driven grain growth, and the corresponding mechanical response showed significant ductility (~20% total strain).[40,60] In contrast, Al thin films that showed limited ductility and relatively high ultimate tensile strengths demonstrated a stable microstructure following fracture as well as no detectable surface evolution, suggesting that deformation and grain growth are necessary conditions for the surface changes.[40,60]

Figs. 1(a) and 1(e) compare the results from MD simulations of strained NC Al with free surfaces with an experimental image of the heavily deformed region of a specimen exhibiting stress-driven grain growth.[63] Despite the difference in mean grain sizes between experiments (~100 nm) and simulations (~14 nm), and that the large strain rate ($3.3 \times 10^8\ s^{-1}$) utilized in simulations is necessarily much higher than in experiments,[68] qualitative agreement was found in the surface topography, which was concentrated near GBs. We note that X-ray diffraction and transmission electron microscopy (TEM) characterization of the sputter-deposited NC Al thin films did not reveal any strong preferred grain orientation,[40] suggesting that comparison with the random grain orientations in the simulated material is reasonable.

Moreover, the calculated surface topography of NC Al containing free surfaces demonstrate similar evolution as a function of deformation in comparison to the experimental surface profiles measured via tapping mode atomic force microscopy (AFM), as shown in Figs. 1(b)–1(d) and 1(f)–1(h). For similar values of total longitudinal strain (along the x direction), a similar trend to those obtained from experiments is observed; namely, increasing surface topography that is concentrated in near GB regions. These results suggest that the presence of a free surface allows for the accommodation of some degree of microstructural evolution.

B. MD simulations of surface evolution and GB motion

Having shown qualitative comparison in surface evolution during tensile testing of NC Al thin films, we now turn our attention to results from MD simulations to glean insight on the underlying mechanisms governing plastic deformation and concomitant surface relief formation. In previous experiments, the surface topography correlated with stress-driven grain growth[63] and was generally consistent with the notion of shear-coupled GB migration.[56,57] The present MD simulations also show substantial microstructural evolution characterized by coupled GB migration and grain annihilation, in addition to other accommodating mechanisms such as dislocation emission and absorption at GBs and GB sliding. Fig. 2 shows a sequence of two distinct sections (cut perpendicular to the surface of the film) as a function of applied longitudinal strain. The top and bottom of the sections are delineated by the free surfaces, which is evident from the coloring of the atoms by the centrosymmetry parameter. In both sections, it is clear that both the surface relief and microstructure evolve during tensile straining, with the latter clearly visualized by overlaying the GBs at different values of total strain [Figs. 2(c) and 2(f)]. The most abrupt surface features appear to be formed at locations where the GB intersects the free surface, or where a GB previously existed and vanished as a result of GB migration in the polycrystal.

Several mechanisms by which GB motion occurred under stress can be identified in the MD simulations and characterized as follows. In the section shown in Figs. 2(a)–2(c), the triple junction formed by GBs A, B, and C migrates upward toward the free surface, leaving little residual content. This occurs by way of migration of GBs A and B toward each other, which proceeds in a "zipping" fashion to align GBs A

[This article is copyrighted as indicated in the article. Reuse of AIP content is subject to the terms at: http://scitation.aip.org/termsconditions. Downloaded to] IP: 128.173.126.47 On: Thu, 07 May 2015 16:31:19

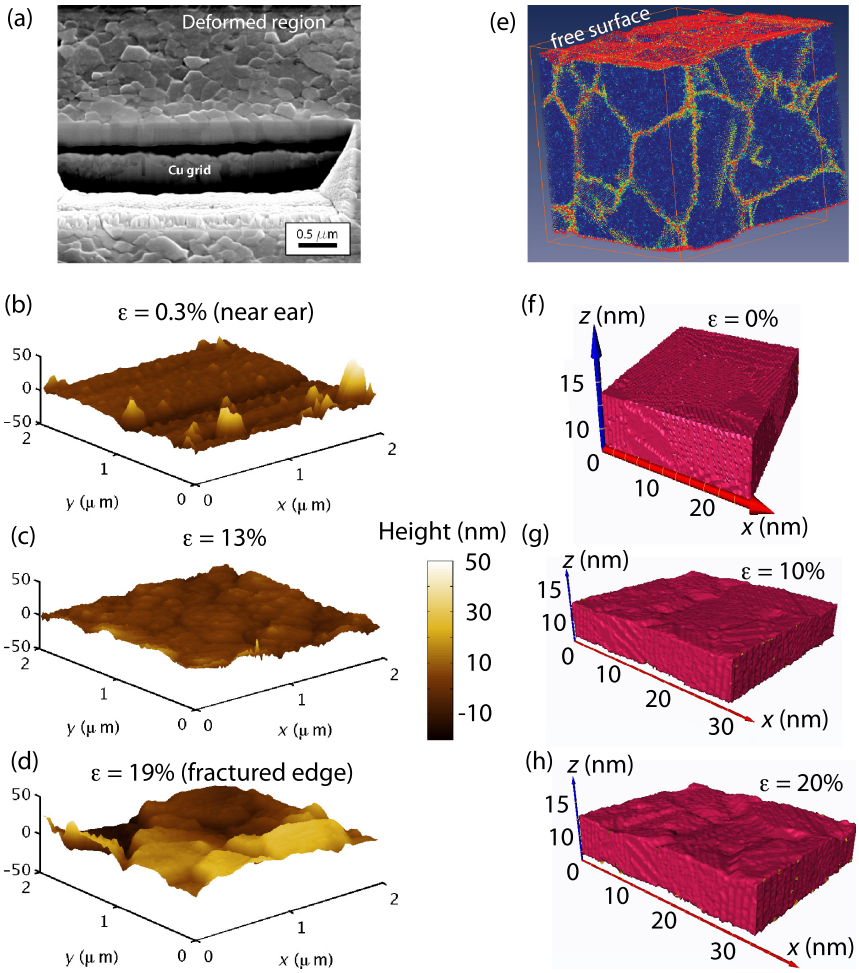

FIG. 1. Surface topography in NC Al thin films due to stress-driven grain growth. (a) SEM image of cross-sectioned thin film near fractured edge of 300 nm thin film deformed to ~20% tensile strain.[63] (b)–(d) AFM images showing evolution of experimentally measured surface topography as a function of axial strain. (e) Detail of the MD simulation after 20% tensile deformation, where the atoms are colored by centrosymmetry parameter, highlighting free surfaces, GBs, and intragranular dislocations. The outline indicates the initial shape of the sample. (f)–(h) Sequences showing surface evolution in MD simulations at similar values of strain. In both cases, the strain is applied along the *x*-direction.

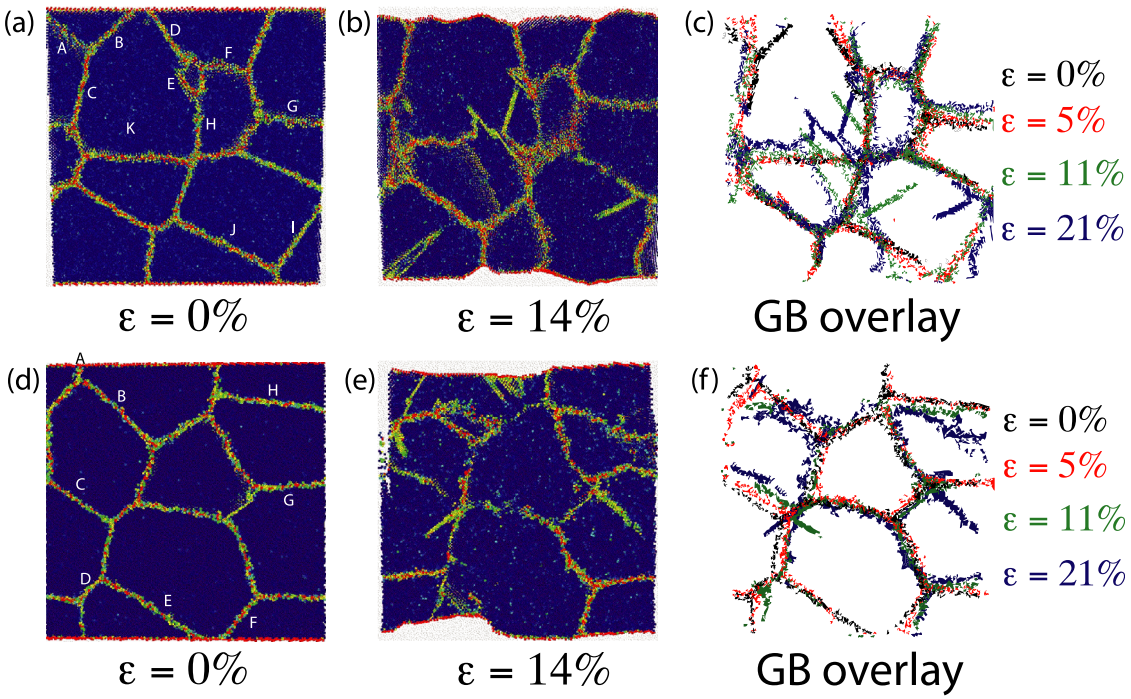

FIG. 2. Details of MD simulations showing microstructural evolution in two cuts perpendicular to the surface of the film. The original configuration for (a) section I and (d) section II is compared to the microstructure at 14% strain (b),(e). Overlays of the GB structure are shown for (c) section I and (f) section II at various values of applied strain, highlighting straight motion and rotation of GBs pinned at triple and quadruple junctions. The coloring of atoms in (a), (b), (d), and (e) corresponds to the centrosymmetry parameter.

[This article is copyrighted as indicated in the article. Reuse of AIP content is subject to the terms at: http://scitation.aip.org/termsconditions. Downloaded to] IP: 128.173.126.47 On: Thu, 07 May 2015 16:31:19

and B with GB C. This process eliminates the grain delineated by GBs A and B and the free surface, and effectively enlarges the neighboring grains. In a similarly configured Y-shaped triple junction given by GBs I and J near the bottom surface, but with the GB perpendicular to the free surface intersecting the surface, the migration of GBs I and J away from each other zips up and eliminates the triple junction at the bottom free surface. As GBs I and J are constrained by the opposite triple junctions in the interior of the film, this migration occurs by translation and rotation, which we term a hinging mechanism. As a result, the slope of the surface shown in this 2D section is both negative and positive, owing to opposite direction of motion of GBs I and J, respectively. This sloped relief is consistent with the production of plastic shear that accompanies motion normal to the GB. In the case where GBs are originally oriented approximately parallel to both surfaces, such as the case of GBs G and K, GB migration is observed towards the free surface, but with relatively low velocities. Additionally, a small grain in the film interior connected by GBs D, E, F, and H was observed to collapse and annihilate at the expense of growth of its neighboring grains. This is consistent with recent *in situ* TEM observations of grain annihilation in nanocrystalline[41] and tricrystalline[69] Al thin films.

A different section cut through the thin film [Figs. 2(d)–2(f)] shows similar zipping (GB A) and hinging (GBs E and F) mechanisms during tensile straining. Surprisingly, while the hinging of GB E about an interior triple junction resulted in a large surface step consistent with a shear-coupled mechanism, GB F was observed to hinge without leaving noticeable surface relief. This suggests that other relaxation mechanisms such as GB sliding or atomic shuffling could be active.[70–72] In addition, the joining of two triple junctions was observed by GB contraction (GB D) to form a quadruple junction. Some sub-surface GBs (G and H) also exhibit hinging, although operation was more difficult due to the microstructural constraint such as triple junctions at the end of these GBs, as discussed later.

Taken as a whole, the operation and efficacy of these mechanisms in promoting microstructural evolution appear to be a function of the local stress state (shear stress at the GB in the case of coupled motion[62]), the specific GB character, the proximity to the free surface, the grain size and topology, and the polycrystal configuration at junctions. The complex interplay of factors leads to the discontinuous nature of stress-driven grain growth, which has been observed experimentally in NC Al thin films.[40] This notion is supported by examining the evolution of normalized grain size during simulated tensile straining, as shown in Fig. 3, where the grain areas of five grains in a section perpendicular to the surface of the film are plotted. That grains both grow and shrink during mechanical loading indicates a competition of processes, which are biased to favor a net growth of polycrystal ensembles.

Detailed examinations of the trajectories of GB atoms confirm that local atomic shuffling and GB sliding sometimes accompanies coupled GB motion in the case of more general GB characters, in contrast to symmetric tilt as is often studied via MD[53–57] and bicrystal experiments.[48–50] For

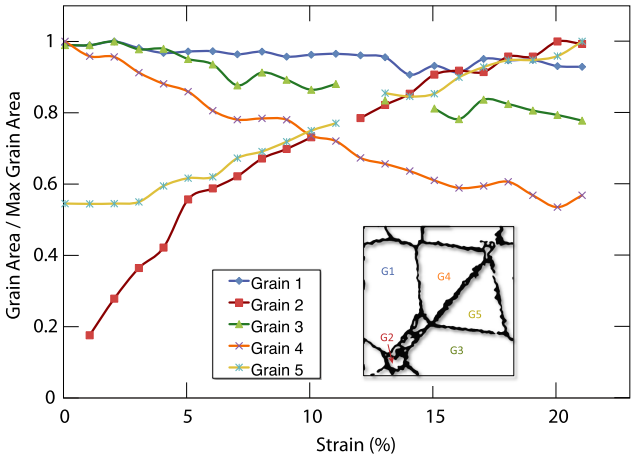

FIG. 3. Normalized grain area computed from MD simulations for several grains identified (inset) in a cut perpendicular to the surface of the film. Both growth and shrinkage of grains are measured, showing a competitive process in the microstructural evolution mediated by GB-specific driving forces and microstructural confinement.

instance, Fig. 4 shows a sequence of a GB delineating a misorientation near $[110]_{upper}//[001]_{lower}$ and $[\bar{1}11]_{upper}//[110]_{lower}$. The GB clearly migrates downward, which is accompanied by shearing along the boundary accomplished by local distortions at the boundary, shuffling of atoms, and direct GB sliding. When this type of stress-driven motion can be accommodated with one end of the GB terminated at the free surface, the result is a shear offset. In addition, such shear offsets resulting from coupled GB motion can be found for embedded GBs, as shown in Fig. 5, where tracking of the same set of atoms during deformation shows the characteristic signature of coupled motion about a likely constrained pivot point.

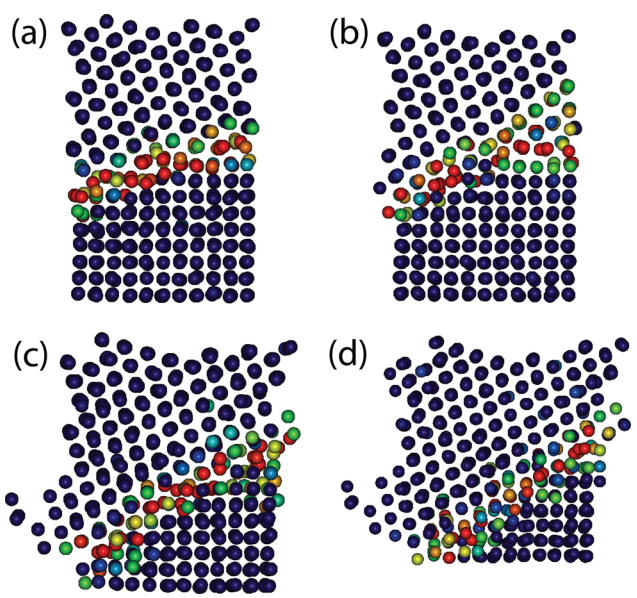

FIG. 4. Detail of the movement of a single GB seen here in a cut perpendicular to the surface of the film. The misorientation of the GB is near $[110]_{upper}//[001]_{lower}$ (perpendicular to the plane of the slice) and $[\bar{1}11]_{upper}//[110]_{lower}$. The coloring of atoms corresponds to the centrosymmetry parameter.

[This article is copyrighted as indicated in the article. Reuse of AIP content is subject to the terms at: http://scitation.aip.org/termsconditions. Downloaded to] IP: 128.173.126.47 On: Thu, 07 May 2015 16:31:19

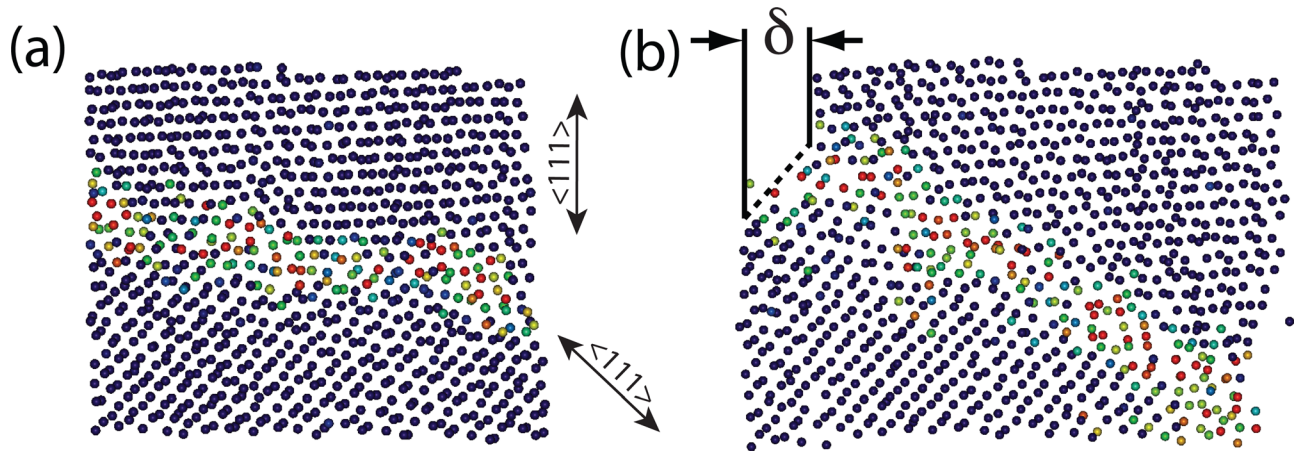

FIG. 5. Detail of the movement of a single embedded GB (envelope of atoms does not represent free surface) seen here in a cut perpendicular to the surface of the film, showing migration and rotation of the GB and the corresponding shear offset. The two pictures correspond to the same group of atoms before and after deformation. While the misorientation relationship for this boundary is not well defined, the arrows indicate ⟨111⟩ type directions in both crystals. The coloring of atoms corresponds to the centrosymmetry parameter.

C. Effects of free surface and microstructural confinement features

In a thin film composed of many grains, surface relief is concentrated near GB regions, as corroborated by experimental observations shown in Fig. 1. One can imagine a scenario where a GB threading the entire film (terminated at both free surfaces) would be driven by a shear stress to migrate laterally and provide surface relief. In the presence of microstructural confinement (as expected in equiaxed NC grain morphologies), however, the GB must migrate by hinging about a less mobile point, such as a triple junction. This rotational motion, as depicted schematically in Fig. 6(a), will still result in plastic shear strain and microstructural evolution, and the magnitude of the surface step is dictated by the coupling factor of the GB and degree of constraint to GB sliding. We find this mechanism reminiscent of single-armed dislocation sources, which also produce plastic shear strain as dislocations rotate around a pinning point on their slip plane (such a mechanism has been shown to be active in μm and sub-μm face-centered cubic single crystals subjected to uniaxial loading[73,74]). However, as the GB character, resolved shear stress on the GB, and the nature of local stress concentrations change, the driving force for this type of GB motion is expected to also vary. This dynamic situation would almost certainly necessitate activity from other strain accommodation mechanisms such as GB sliding[57,70] and partial dislocation nucleation and absorption.[14,17] Experimental support for this mechanism can be found via AFM measurements of GB terracing in deformed NC thin films, as shown in Fig. 6(b), where distinct steps with roughly self-similar profiles were observed in the vicinity of GBs. In these cases, it appears as if GBs have not only shifted out-of-plane, but also have left a trace of sheared region along the surface of the film. We hypothesize that the experimental observation of stepped profiles exhibiting self-similarity, which combine lateral and out-of-plane motion of the GBs, can be rationalized by considering the surface impression as traces of the GB that penetrate the thin native oxide layer at different times when the vertical motion is sufficiently large to break through the oxide.

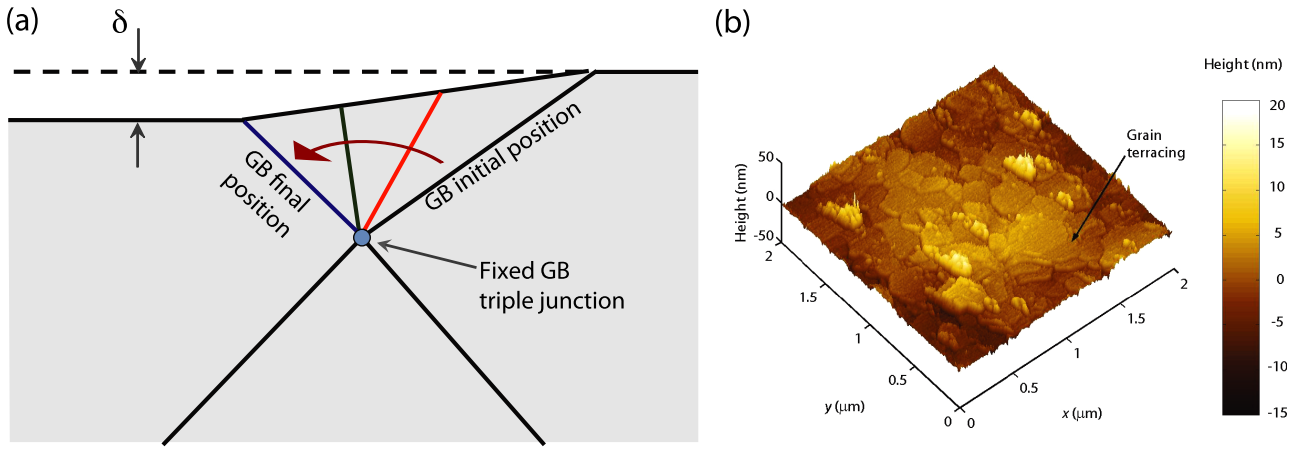

FIG. 6. (a) Proposed mechanism of constrained coupled GB motion as identified in MD simulations. A fixed GB triple junction provides the pinned constraint of a GB subjected to a shear stress driving force moves by rotation about the pinning point. Coupled motion of a GB intersecting free surface results in shearing and topography evolution characterized by a surface offset δ. (b) AFM height image of a deformed 300 nm film near the fractured edge, showing relative motion of adjacent grains and terracing of individual grains.

[This article is copyrighted as indicated in the article. Reuse of AIP content is subject to the terms at: http://scitation.aip.org/termsconditions. Downloaded to] IP: 128.173.126.47 On: Thu, 07 May 2015 16:31:19

To elucidate the effect of microstructural confinement on subsequent evolution, we performed MD simulations of an identical NC microstructure but with the free surface in different positions. Examining the evolution of a section parallel to the free surface at a distance $\lambda = 14$ nm [Figs. 7(a)–7(d)], and subsequently "polishing" the surface back to give a smaller distance to the section of $\lambda = 2$ nm [Figs. 7(e)–7(h)], enabled facile comparison. Sequences showing the progression of applied tensile strain for $\varepsilon = 0$, 7, and 14% are shown in Figs. 7(b)–7(d) and 7(f)–7(h) for $\lambda = 14$ nm and $\lambda = 2$ nm, respectively. One salient observation evident from these results is that the evolution of two relatively small grains (G1 and G2) differs depending on the proximity to the free surface. Up to 7% strain, small changes to these grain shapes occur in both cases, most notably to G2. However, at larger strains, G1 begins to shrink somewhat uniformly when it is closer to the free surface [Fig. 7(h)], while remaining stable when it is embedded deeper in the film [Fig. 7(d)]. In contrast, grain G2 appears to undergo more pronounced shape changes when it is deeper in the film [Fig. 7(d)], although copious dislocation activity is observed on the leftmost GB, which could contribute to the apparent local disorder. Also noteworthy is that the near collapse of G1 at high strain when $\lambda = 2$ nm [Fig. 7(h)] results in the disintegration of a high-angle GB between G4 and G5 (originally given by the junction of G1, G3, G4, and G5), promoting grain growth of the nanocrystalline structure. These results suggest that stress-driven grain growth is somewhat inhibited, although not entirely suppressed, when microstructural confinement from neighboring grains is present.

In addition to microstructural and topological constraints to stress-driven grain growth, it is known that solutes and second-phase particles can provide energetic[33–36] and kinetic[29–32] barriers to GB migration. It is thus instructive to examine the relative efficacy of segregated solutes at GBs vs. the microstructural confinement examined previously. Figs. 7(i)–7(l) shows the same section at the smaller distance to the free surface ($\lambda = 2$ nm), but with 1 at. % H atoms decorating the GBs. Comparing these results to the section of the pure Al at $\lambda = 2$ nm shows that, despite the near proximity to the free surface, the presence of H at the GBs serves to mostly suppress GB migration under stress. Indeed, most shape changes to grains that are evident in Figs. 7(j)–7(l) are the result of dislocation nucleation and absorption at GBs, which appear to be a primary plasticity mechanism in concert with some GB sliding. This result is consistent with experimental

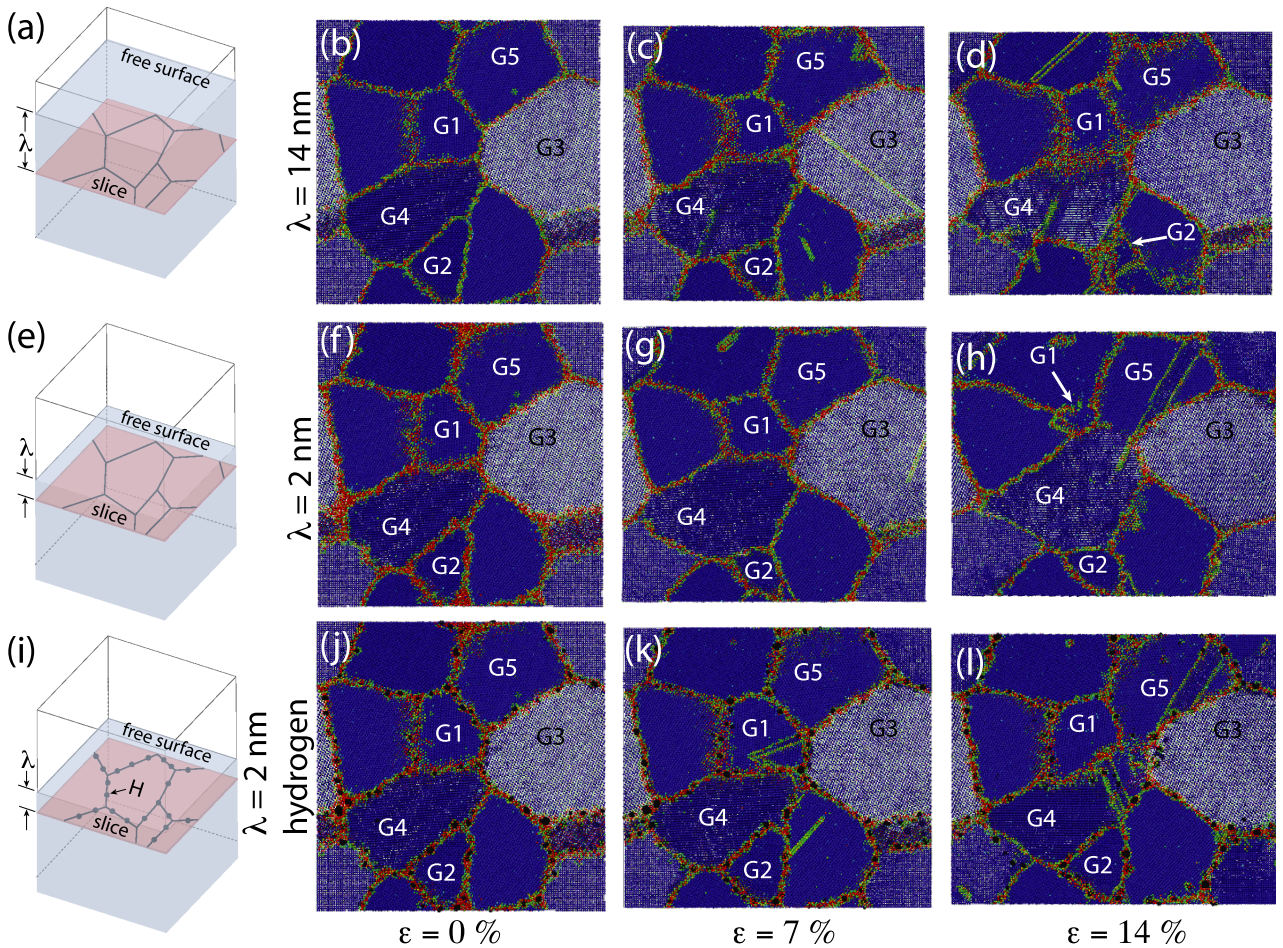

FIG. 7. Efficacy of microstructural confinement and GB pinning by impurities in hindering microstructural evolution. (a)–(d) The sequence of GB motion (at 0, 7, and 14% applied strain) in a cut parallel to and 14 nm below the free surface shows a lesser extent of grain growth compared to the identical cut only 2 nm below the surface (e)–(h). At the same distance to the free surface ($\lambda = 2$ nm), the same cut shows very little GB motion when 1 at. % H impurities (black atoms) are placed at the GBs (i)–(l), which effectively hinder stress-driven GB motion. The different shades of blue apparent in the various grains arise from the differences in projected atomic density associated with each grain orientation.

[This article is copyrighted as indicated in the article. Reuse of AIP content is subject to the terms at: http://scitation.aip.org/termsconditions. Downloaded to] IP: 128.173.126.47 On: Thu, 07 May 2015 16:31:19

measurements[60,61] and MD simulations[75] of NC Al-O alloys showing that a critical concentration of O solute at GBs can increase the critical stress required for stress-driven GB migration and suppress grain growth, resulting in dramatically different mechanical response of NC Al films.

IV. DISCUSSION

A. Comparison of surface topography between experiments and simulation

MD simulations and similar experiments demonstrate a correlation between microstructural evolution and surface topography evolution during tensile straining of NC Al thin films, the extent of which scales with the progression of deformation (see Fig. 1). In contrast to characteristics of surface roughening during severe plastic deformation of ductile metals (e.g., during sheet forming and extrusion) that often exhibit mesoscopic roughness morphology due to the accumulation and accommodation of crystalline slip bands,[76–79] the surface relief we observed was directly tied to motion of GBs. This highlights the surface morphology as a useful signature of subsurface microstructural evolution. Qualitative agreement between the surface evolution observed in MD and that in experiment exists as evidenced by surface steps at GBs and grain rotations. Whilst direct quantitative comparisons are more difficult due to the differences in grain sizes and testing strain rates, we estimated the mean surface roughness normalized by the mean initial grain size d. Interestingly, we obtain surface roughness values of approximately $0.1d$ and $0.4d$ at axial strains of 12% and 20%, respectively, in both experiment and MD simulations. This suggests that the magnitude of surface topography that results from microstructural evolution is proportional to the microstructural length scales present in the thin films. This is consistent with the MD study by Derlet and Van Swygenhoven on the role of the surface in affecting plastic response in NC metals.[80] They reported increased GB sliding and dislocation activity in near-surface regions and estimated the extent of the surface influence to be of the order of the grain size. A complementary study by Li *et al.* reported on ambient and high temperature MD simulations of NC Al with free surfaces to study the effect of heterogeneous residual strains and plastic strain recovery.[81] While these authors did not focus on surface topography evolution, surfaces were shown to roughen following deformation in regions concentrated near GB/free surface intersections, as attributed to GB sliding, GB diffusion, and dislocation slip. Fractional strains due to GB and dislocation processes were computed, where it was shown that GB diffusion and sliding processes dominate at high temperature and small grain sizes. However, any plastic strain resulting from coupled GB motion was not incorporated in these calculations (coupled GB motion is indeed a vehicle for producing plastic strain) and in our simulations and experiments could provide a non-negligible amount of strain.

B. Grain boundary motion as a function of the proximity to free surface

Analogous to the simulations of Derlet and Van Swygenhoven,[80] we observe more stress-driven GB motion (in an identical microstructure at a given strain) when it is closer to the free surface, consistent with reports of higher GB velocities in simulated microstructures with free surfaces.[82] However, the more constrained microstructure (i.e., buried) also exhibited increased dislocation activity in the form of partial dislocations nucleating at one GB and traversing the grain unimpeded. In certain grains (e.g., G2 in Fig. 7), the accommodation of such lattice strain resulted in substantial changes to grain shapes. Our results suggest that the potency of the free surface effect is noticeable when the GB network is within a distance λ approximately equal to a grain diameter d. Given a fixed specimen thickness t, one would expect that the influence of GB motion on the mechanical response would increase with increasing d assuming the same underlying deformation mechanisms. Clearly, the role of the free surface should be important when $t \approx d$ (e.g., columnar or bamboo microstructures), and the limit of $t/d \rightarrow \infty$ represents a bulk nanostructured material, where the enhancement of GB motion owing to the presence of the free surface would be minimal. Nevertheless, stress-driven grain growth in bulk nanostructured metals at low homologous temperatures has been experimentally observed and shown to affect mechanical properties,[40] emphasizing that microstructural constraint alone is not sufficient to fully suppress such mechanisms. Thus, modeling efforts for stress-driven GB motion should include a material core governed by constraints, yet still able to evolve under stress, and a shell with enhanced mobility.

In the framework of the theory of coupled GB motion presented by Cahn and Taylor,[57] corroborated with MD simulations of symmetric tilt GBs for a large range of misorientations,[53–55] one can envision a simplified picture of microstructural constraint on the kinetic relationships for GBs. As postulated by Cahn and Taylor, the tangential velocity of a GB $v_{||}$ can be written as $v_{||} = \beta v_n + v_s$, where β is the GB coupling factor, v_n is the velocity of normal motion of the GB, and v_s is the velocity due to tangential sliding alone. In the situation of pure coupled motion (i.e., $v_s = 0$), then $v_{||} = \beta v_n$ and any normal motion of the GB requires simultaneous tangential motion, the degree of which depends on the coupling factor β (a function of tilt misorientation). A situation such as this is plausible for a properly oriented tilt GB near a free surface, such as depicted in Fig. 6. If one end of the GB would be pinned, then the kinetics of the GB motion under a constant driving force would be governed by the changes in GB misorientation (and hence β) during the pivoting motion. However, provided a GB and local environment not favorable for free coupled motion (e.g., due to stress heterogeneities, microstructural constraints, etc.) where GB sliding occurs, then $v_s > 0$ and hence $v_n < v_{||}/\beta$. Thus, the normal motion of the GB could be reduced by the action of GB sliding, which we have shown here to be affected by the presence (and absence) of a free surface in close proximity. Note that a reduction in β is not required to reduce GB normal motion, as confirmed by Velasco *et al.*[64] This simple analysis would also apply to different configurations of GB networks within bulk polycrystals with varying degrees of constraint.

Indeed, Trautt and Mishin recently used MD to study the shrinkage of an isolated cylindrical grain under capillary-based

[This article is copyrighted as indicated in the article. Reuse of AIP content is subject to the terms at: http://scitation.aip.org/termsconditions. Downloaded to] IP: 128.173.126.47 On: Thu, 07 May 2015 16:31:19

driving forces and corresponding grain rotation.[72] In particular, these authors investigated the effect of imposed constraints (preventing grain rotation or by applying an opposing torque), which altered the observed kinetics of GB motion. They found that in a curved GB geometry, GB coupled motion is always accompanied by some extent of GB sliding. In addition, the effect of constraint led to reductions in GB motion due to the difficult of GB sliding. Based on our results, the degree of GB retardation would depend on a complex interplay of GB character, grain topology, microstructural constraining features (e.g., triple and quadruple points), and chemical environment at the GB. We also note that the analysis and MD simulations analyzing coupled GB motion have typically been performed on symmetrical tilt GBs; while in a realistic polycrystal, one would expect a larger diversity of GB types. For instance, any twist component of a GB is not expected to lead to coupled motion.[57] We note the recent experiments of Mompiou *et al.*, who reported *in situ* TEM observations of shrinkage of isolated grains in tricrystalline Al when heated to temperatures between 250 and 400 °C, where no rotation was measured.[69] In these experiments, the normal motion of the GB was attributed to atomic shuffling owing to a low coupling factor.

C. Pinning effect of impurities located at grain boundaries

The hindrance of stress-driven GB motion due to the presence of impurity atoms would be expected to play a role in the measured mechanical response via the possible roles of solid solution strengthening effects,[83,84] GB pinning leading to increased critical stresses for coupled motion,[75,85] and differences in local atomic environment affecting GB dislocation nucleation, propagation, and absorption. Tang *et al.* recently showed that classical solid strengthening effects cannot alone explain the strengthening observed in nanocrystalline Al thin films, suggesting that the increased stress threshold for GB motion was instead responsible for the measured strengthening.[61] These experimental observations corroborate MD simulations performed by Elsener *et al.*[75] of coupled motion of a single symmetric tilt GB with O solutes in its path. These results showed a linear relationship between the critical stress for GB motion and interfacial excess of solute. Additional strengthening effects due to solute atoms at GBs in nanocrystalline metals have been measured by Rupert *et al.* in Ni-W alloys, which were attributed to the a global effect of solutes interacting with dislocations pinned by GBs and subjected to shear stresses.[86] Fig. 8 compares the tensile stress strain response of our MD simulations in the absence and presence of H solutes with experimentally measured curves of pure Al and Al-O thin films. The experimental stress strain curves were reported in a previous publication where the O was quantified by 3D atom probe tomography and shown to segregate to GBs.[61] Despite the large differences in grain size, imposed strain rate, and solute species in experiment and simulation, several similarities yet exist. First, the yield and flow stresses are comparable, ranging from approximately 200–300 MPa. Second, the large initial work hardening rate is followed by a relatively sharp upper yield point, being more pronounced in the experimental Al-O and simulated thin films. Additionally, adding solute atoms to the GB has the net effect of strengthening the material, which is consistent with the hindrance of stress-driven grain growth as shown above and before.[61]

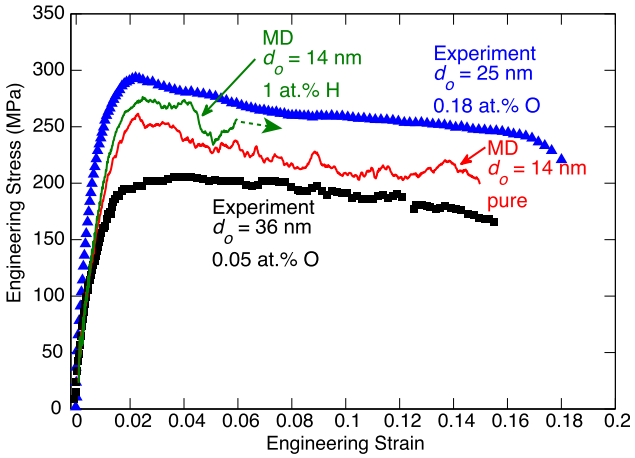

FIG. 8. Tensile stress-strain curves for MD simulations of Al thin films with and without H solute atoms at the GBs. These curves are compared to experimentally measured behavior of Al-O nanocrystalline thin films deposited at different base pressures leading to different concentrations of O solute,[61] which were shown to undergo stress-driven grain growth.

V. CONCLUSIONS

Using MD simulations in comparison to relevant experimental data and observations, we have studied the effect of microstructural and chemical constraints on room temperature stress-driven GB motion and grain growth in NC Al thin films. The following conclusions can be drawn:

(1) Both simulated and experimental tensile testing of nominally pure NC Al thin films lead to stress-driven GB motion and grain growth. In our thin film geometry, these mechanisms lead to surface topography evolution as manifested by step heights at GBs and grain rotation. Despite differences in initial mean grain size and imposed strain rates, good agreement is found for the magnitude of surface roughening normalized by initial grain size at a given strain.
(2) The GB motion is driven by shear stresses along the GB and is shown to occur by both coupled GB motion and GB sliding. The proximity of the free surface to identical microstructural sections has a substantial effect on the ensuing microstructural evolution, particularly at depths below the free surface equal to approximately d. GBs that terminate at the free surface on one end show increased normal motion as well as sliding in comparison to a buried GB, although local constraints can enhance dislocation activity, which provide an additional accommodation mechanism. Whereas the degree of sliding changes with the buried depth of GBs, the coupling factors are not affected by the constraint and only change if the GB character evolves during motion.
(3) In addition to microstructural constraints, local pinning of GBs by solute impurities effectively impedes GB motion. The altered atomic environment resulting from

[This article is copyrighted as indicated in the article. Reuse of AIP content is subject to the terms at: http://scitation.aip.org/termsconditions. Downloaded to] IP: 128.173.126.47 On: Thu, 07 May 2015 16:31:19

solutes in the GB may provide both kinetic and energetic factors for controlling GB motion. In addition, nucleation and absorption of partial dislocations at GBs appears to be affected by the presence of solutes.

Taken as a whole, our results show that stress-driven microstructural evolution in NC Al is strongly affected by microstructural and chemical constraints inherent to any realistic ensemble of nanocrystallites with large volumes of interfacial material. The presence of free surfaces can relax some of this constraint owing to the lack of strain compatibility and change the resulting evolution. Future modelling efforts aimed at predictive capability of stress-driven microstructural evolution should incorporate the microstructural complexity of NC metals, which may be aided by advanced three-dimensional characterization techniques offering information regarding morphology, crystalline orientation, chemistry, and structure.[87,88]

ACKNOWLEDGMENTS

This work was supported by the National Science Foundation (NSF) Materials Network Program, Grant No. DMR-1008222. D.S.G. acknowledges additional support through start-up funding from the University of Pennsylvania. We thank K. J. Hemker for fruitful discussions.

[1]K. S. Kumar, H. Van Swygenhoven, and S. Suresh, Acta. Mater. **51**, 5743 (2003).
[2]M. A. Meyers, A. Mishra, and D. J. Benson, Prog. Mater. Sci. **51**, 427 (2006).
[3]M. Dao, L. Lu, R. J. Asaro, J. T. M. De Hosson, and E. Ma, Acta. Mater. **55**, 4041 (2007).
[4]K. Lu, L. Lu, and S. Suresh, Science **324**, 349 (2009).
[5]Y. Wang, M. Chen, F. Zhou, and E. Ma, Nature **419**, 912 (2002).
[6]X. X. Huang, N. Hansen, and N. Tsuji, Science **312**, 249 (2006).
[7]P. G. Sanders, J. A. Eastman, and J. R. Weertman, Acta. Mater. **45**, 4019 (1997).
[8]J. Schiøtz and K. W. Jacobsen, Science **301**, 1357 (2003).
[9]K. S. Kumar, S. Suresh, M. F. Chisholm, J. A. Horton, and P. Wang, Acta. Mater. **51**, 387 (2003).
[10]Z. Budrovic, H. Van Swygenhoven, P. M. Derlet, S. Van Petegem, and B. Schmitt, Science **304**, 273 (2004).
[11]E. O. Hall, Proc. Phys. Soc. London, Sect. B **64**, 747 (1951).
[12]N. J. Petch, J. Iron Steel Inst., London **174**, 25 (1953).
[13]V. Yamakov, D. Wolf, S. R. Phillpot, A. K. Mukherjee, and H. Gleiter, Nature Mater. **1**, 45 (2002).
[14]H. Van Swygenhoven, P. M. Derlet, and A. Hasnaoui, Phys. Rev. B **66**, 024101 (2002).
[15]M. Chen, E. Ma, K. J. Hemker, H. Sheng, Y. Wang, and X. Cheng, Science **300**, 1275 (2003).
[16]D. Wolf, V. Yamakov, S. R. Phillpot, A. K. Mukherjee, and H. Gleiter, Acta. Mater. **53**, 1 (2005).
[17]H. Van Swygenhoven, P. M. Derlet, and A. G. Frøseth, Acta. Mater. **54**, 1975 (2006).
[18]L. Lu, X. Chen, X. Huang, and K. Lu, Science **323**, 607 (2009).
[19]B. S. Günther, A. Kumpmann, and H. D. Kunze, Scr. Metall. Mater. **27**, 833 (1992).
[20]V. Y. Gertsman and R. Birringer, Scr. Metall. Mater. **30**, 577 (1994).
[21]T. R. Malow and C. C. Koch, Mater. Sci. Forum **225**, 595 (1996).
[22]J. A. Haber and W. E. Buhro, J. Am. Chem. Soc. **120**, 10847 (1998).
[23]A. J. Haslam, S. R. Phillpot, D. Wolf, D. Moldovan, and H. Gleiter, Mater. Sci. Eng. A **318**, 293 (2001).
[24]M. Ames, J. Markmann, R. Karos, A. Michels, A. Tschöpe, and R. Birringer, Acta. Mater. **56**, 4255 (2008).
[25]F. Zhou, J. Lee, S. Dallek, and E. J. Lavernia, J. Mater. Res. **16**, 3451 (2001).
[26]Y. M. Wang, S. Cheng, Q. M. Wei, E. Ma, T. G. Nieh, and A. Hamza, Scr. Mater. **51**, 1023 (2004).
[27]C. C. Koch, R. O. Scattergood, K. A. Darling, and J. E. Semones, J. Mater. Sci. **43**, 7264 (2008).
[28]T. Frolov, K. A. Darling, L. J. Kecskes, and Y. Mishin, Acta Mater. **60**, 2158 (2012).
[29]C. S. Smith, Trans. AIME **175**, 15 (1948).
[30]J. W. Cahn, Acta Metall. **10**, 789 (1962).
[31]T. R. Malow and C. C. Koch, Acta Mater. **45**, 2177 (1997).
[32]A. Michels, C. E. Krill, H. Ehrhardt, R. Birringer, and D. T. Wu, Acta Mater. **47**, 2143 (1999).
[33]J. Weissmuller, Nanostruct. Mater. **3**, 261 (1993).
[34]R. Kirchheim, Acta Mater. **50**, 413 (2002).
[35]P. C. Millett, R. P. Selvam, and A. Saxena, Acta Mater. **55**, 2329 (2007).
[36]J. R. Trelewicz and C. A. Schuh, Phys. Rev. B **79**, 094112 (2009).
[37]M. Jin, A. M. Minor, E. A. Stach, and J. W. Morris, Acta Mater. **52**, 5381 (2004).
[38]K. Zhang, J. R. Weertman, and J. A. Eastman, Appl. Phys. Lett. **87**, 061921 (2005).
[39]G. J. Fan, L. F. Fu, H. Choo, P. K. Liaw, and N. D. Browning, Acta Mater. **54**, 4781 (2006).
[40]D. S. Gianola, S. Van Petegem, M. Legros, S. Brandstetter, H. Van Swygenhoven, and K. J. Hemker, Acta Mater. **54**, 2253 (2006).
[41]M. Legros, D. S. Gianola, and K. J. Hemker, Acta Mater. **56**, 3380 (2008).
[42]D. Pan, S. Kuwano, T. Fujita, and M. W. Chen, Nano Lett. **7**, 2108 (2007).
[43]S. Brandstetter, K. Zhang, A. Escuadro, J. R. Weertman, and H. Van Swygenhoven, Scr. Mater. **58**, 61 (2008).
[44]R. A. Meirom, D. H. Alsem, A. L. Romasco, T. Clark, R. G. Polcawich, J. S. Pulskamp, M. Dubey, R. O. Ritchie, and C. L. Muhlstein, Acta Mater. **59**, 1141 (2011).
[45]C. H. Li, E. H. Edwards, J. Washburn, and E. R. Parker, Acta Metall. **1**, 223 (1953).
[46]D. W. Bainbridge, C. H. Li, and E. H. Edwards, Acta Metall. **2**, 322 (1954).
[47]W. T. Read and W. Shockley, Phys. Rev. **78**, 275 (1950).
[48]M. Winning, G. Gottstein, and L. S. Shvindlerman, Acta Mater. **49**, 211 (2001).
[49]M. Winning, G. Gottstein, and L. S. Shvindlerman, Acta Mater. **50**, 353 (2002).
[50]M. Winning and A. D. Rollett, Acta Mater. **53**, 2901 (2005).
[51]F. Mompiou, D. Caillard, and M. Legros, Acta Mater. **57**, 2198 (2009).
[52]D. Caillard, F. Mompiou, and M. Legros, Acta Mater. **57**, 2390 (2009).
[53]F. Sansoz and J. F. Molinari, Acta Mater. **53**, 1931 (2005).
[54]V. A. Ivanov and Y. Mishin, Phys. Rev. B **78**, 064106 (2008).
[55]L. Wan and S. Q. Wang, Phys. Rev. B **82**, 214112 (2010).
[56]J. W. Cahn and J. E. Taylor, Acta Mater. **52**, 4887 (2004).
[57]J. W. Cahn, Y. Mishin, and A. Suzuki, Acta Mater. **54**, 4953 (2006).
[58]T. Gorkaya, D. A. Molodov, and G. Gottstein, Acta Mater. **57**, 5396 (2009).
[59]G. Gottstein, A. H. King, and L. S. Shvindlerman, Acta Mater. **48**, 397 (2000).
[60]D. S. Gianola, B. G. Mendis, X. M. Cheng, and K. J. Hemker, Mater. Sci. Eng. A **483–484**, 637 (2008).
[61]F. Tang, D. S. Gianola, M. P. Moody, K. J. Hemker, and J. M. Cairney, Acta Mater. **60**, 1038 (2012).
[62]T. J. Rupert, D. S. Gianola, Y. Gan, and K. J. Hemker, Science **326**, 1686 (2009).
[63]D. S. Gianola, C. Eberl, X. M. Cheng, and K. J. Hemker, Adv. Mater. **20**, 303 (2008).
[64]M. Velasco, H. Van Swygenhoven, and C. Brandl, Scr. Mater. **65**, 151 (2011).
[65]S. Plimpton, J. Comput. Phys. **117**, 1 (1995).
[66]H. Van Swygenhoven, D. Farkas, and A. Caro, Phys. Rev. B **62**, 831 (2000).
[67]M. Ruda, D. Farkas, and J. Abriata, Phys. Rev. B **54**, 9765 (1996).
[68]C. Deng and C. A. Schuh, Phys. Rev. B **84**, 214102 (2011).
[69]F. Mompiou, M. Legros, T. Radetic, U. Dahmen, D. S. Gianola, and K. J. Hemker, Acta Mater. **60**, 2209 (2012).
[70]H. Van Swygenhoven and P. M. Derlet, Phys. Rev. B **64**, 224105 (2001).
[71]D. Farkas, A. Frøseth, and H. Van Swygenhoven, Scr. Mater. **55**, 695 (2006).
[72]Z. T. Trautt and Y. Mishin, Acta Mater. **60**, 2407 (2012).
[73]S. H. Oh, M. Legros, D. Kiener, and G. Dehm, Nature Mater. **8**, 95 (2009).

[This article is copyrighted as indicated in the article. Reuse of AIP content is subject to the terms at: http://scitation.aip.org/termsconditions. Downloaded to] IP: 128.173.126.47 On: Thu, 07 May 2015 16:31:19

[74]F. Mompiou, M. Legros, A. Sedlmayr, D. S. Gianola, D. Caillard, and O. Kraft, Acta Mater. **60**, 977 (2012).
[75]A. Elsener, O. Politano, P. M. Derlet, and H. Van Swygenhoven, Acta Mater. **57**, 1988 (2009).
[76]Y. Z. Dai and F. P. Chiang, Mech. Mater. **13**, 55 (1992).
[77]W. Tong, L. G. Hector, H. Weiland, and L. F. Wieserman, Scr. Mater. **36**, 1339 (1997).
[78]Y. S. Choi, H. R. Piehler, and A. D. Rollett, Metall. Mater. Trans. A **35**, 513 (2004).
[79]Z. Zhao, R. Radovitzky, and A. Cuitino, Acta Mater. **52**, 5791 (2004).
[80]P. M. Derlet and H. Van Swygenhoven, Philos. Mag. A **82**, 1 (2002).
[81]X. Li, Y. Wei, W. Yang, and H. J. Gao, Proc. Natl. Acad. Sci. U.S.A. **106**, 16108 (2009).
[82]D. Farkas, S. Mohanty, and J. Monk, Mater. Sci. Eng. A **493**, 33 (2008).
[83]R. L. Fleischer, in *The Strengthening of Metals*, edited by D. Peckner (Reinhold, New York, 1964).
[84]R. Labusch, Phys. Status Solidi **41**, 659 (1970).
[85]J. Schäfer and K. Albe, Scr. Mater. **66**, 315 (2012).
[86]T. J. Rupert, J. C. Trenkle, and C. A. Schuh, Acta Mater. **59**, 1619 (2011).
[87]E. A. Marquis and J. M. Hyde, Mater. Sci. Eng. R **69**, 37 (2010).
[88]S. Zaefferer, Cryst. Res. Technol. **46**, 607 (2011).

[This article is copyrighted as indicated in the article. Reuse of AIP content is subject to the terms at: http://scitation.aip.org/termsconditions. Downloaded to] IP: 128.173.126.47 On: Thu, 07 May 2015 16:31:19